A Global Data Record of Daily Landscape Freeze/Thaw status
Version 4.0

Contact Information:

Youngwook Kim, John S. Kimball, Jinyang Du. and Joseph Glassy

Numerical Terradynamic Simulation Group (NTSG)

The University of Montana

Missoula MT, 59812

Email: john.kimball@umontana.edu; youngwook.kim@umontana.edu;

Jinyang.du@umontana.edu; um.glassy@gmail.com

Project URL: http://freezethaw.ntsg.umt.edu/

Release date: 2017-08-09T16:47:00

The following reference should be used to cite these data:

Kim, Y., J. S. Kimball, J. Du, and J. Glassy. 2017. MEaSUREs Global Record of Daily Landscape Freeze/Thaw Status, Version 04 [1979 to 2016]. Boulder Colorado USA: National Snow and Ice Data Center. Digital media (http://dx.doi.org/10.5067/MEASURES/CRYOSPHERE/nsidc-0477.004).

The following peer-reviewed citation provides a detailed description of the FT-ESDR

algorithms, accuracy and performance, and science applications:

Kim, Y., J. S. Kimball, J. Glassy, and J. Du. (2017). An Extended Global Earth System Data Record on Daily Landscape Freeze-Thaw Determined from Satellite Passive Microwave Remote Sensing, *Earth System Science Data*, 9 (1), 133-147.

Contents:

I. Introduction:

This document describes a global data record of daily landscape Freeze/Thaw (FT) status derived from satellite passive microwave remote sensing. The FT state parameter quantifies the predominant frozen or non-frozen state of the landscape and is closely linked to changes in the surface energy budget and evapotranspiration (Zhang et al. 2011), vegetation growth and phenology (Kim et al., 2014b), snowmelt dynamics (Kim et al., 2015), permafrost extent and stability (Park et al., 2016), terrestrial carbon budgets and land-atmosphere trace gas exchange (Kim et al., 2014a). Satellite microwave remote sensing is well suited for global FT monitoring due to its relative insensitivity to atmospheric contamination and solar illumination effects, and strong microwave sensitivity to changes in surface dielectric properties between frozen and non-frozen conditions.

II. Data description

The current FT Earth System Data Record (FT-ESDR) was primarily derived using similar calibrated overlapping daily [morning (AM) and afternoon (PM) overpass] radiometric brightness temperature (T_b) measurements at 37 GHz (V-pol) frequency from the Scanning

Multichannel Microwave Radiometer (SMMR), Special Sensor Microwave Imager (SSM/I) and SSM/I Sounder (SSMIS) sensor series. The resulting FT-ESDR represents a consistent, daily FT global record that extends over a 38 year (1979 to 2016) observation period, ensuring cross-sensor consistency through pixel-wise adjustment of the SMMR T_b record based on empirical analyses of overlapping SMMR and SSM/I T_b measurements (Kim et al. 2012).

The FT-ESDR also includes a synergistic global daily FT product derived from NASA AMSR-E (Advanced Microwave Scanning Radiometer for EOS) daily (AM and PM overpass) 36.5 GHz (V-pol) T_b retrievals (June 2002 to September 2011), which were extended to 2016 using similar T_b measurements from the Japan Aerospace Exploration Agency (JAXA) Advanced Microwave Scanning Radiometer 2 (AMSR2) sensor record. Double-differencing calibration of AMSR2 to AMSR-E T_b records were conducted using similar frequency collocated overlapping T_b records from the FY-3B Microwave Radiation Imager (MWRI), which was applied to fill the temporal T_b gaps for 2011-2012 period (Du et al., 2014). The MWRI on the Chinese FengYun 3B (FY3b) satellite was launched in November 2010 (Yang et al., 2011) and has similar instrument configuration and data acquisition times as the AMSR-E and AMSR2 (hereafter AMSR) sensors. The SMMR, SSM/I, and AMSR components of the FT-ESDR are fully compatible, with similar T_b frequency FT retrievals, consistent projection and product formats, and extending over the same global domain. Calibrated, overlapping T_b data records from SMMR (Knowles et al. 2000), SSM/I and SSMIS (RSS V.7, Armstrong et al. 1998), and AMSR-E (RSS V.6, Knowles et al. 2006) sensors were used to assemble the FT-ESDR. AMSR2 L1R swath T_b data (Imaoka et al., 2012) obtained from the JAXA were re-projected to a 25-km global EASE-Grid 1.0 projection format using an Inverse Distance Squared spatial interpolation approach following previously established methods (Armstrong and Brodzik, 1995; Du et al., 2014). Detailed descriptions of the FT-ESDR methods, algorithm performance and product accuracy are provided by Kim et al. (2017). A related AMSR global land parameter data record for ecosystem studies includes a FT-ESDR derived frozen flag used for the retrieval of higher order land parameters (Du et al., 2015; Jones and Kimball 2012).

The FT-ESDR is intended to have sufficient accuracy, resolution, and coverage to resolve physical processes linking Earth's water, energy and carbon cycles. The product is designed to

determine the FT status of the composite landscape vegetation-snow-soil medium to a sufficient level to characterize the frozen temperature constraints to surface water mobility, vegetation productivity, ecosystem respiration and land-atmosphere carbon (CO_2) fluxes. The FT-ESDR utilizes a daily binary FT state classification on a grid cell-by-cell basis, posted to a global 25km Earth grid. The FT classification algorithm uses a temporal change detection of radiometric T_b time-series that identify FT transition sequences by exploiting the dynamic temporal T_b response to differences in the aggregate landscape dielectric constant that occur as the landscape transitions between predominantly frozen and non-frozen conditions (McDonald and Kimball 2005; Kim et al., 2011, 2012). Satellite ascending and descending orbital data time series are processed separately to produce information on AM, PM and composite daily FT conditions (CO). Additional variables distinguished by the FT-ESDR include transitional (AM frozen and PM thawed) or inverse transitional (AM thawed and PM frozen) conditions. **Table 2** describes the file encoding of FT-ESDR pixel values corresponding to frozen, thawed, and transitional conditions. The FT-ESDR global domain encompasses all land areas affected by seasonal frozen temperatures, including urban, barren land, snow-ice and open water body dominant grid cells (Kim et al., 2017).

The FT-ESDR data are available for public access via FTP download through the FT-ESDR project web site (http://freezethaw.ntsg.umt.edu) and NTSG HTTP Data Service (http://luna.ntsg.umt.edu/data/FT_ESDR/), and through the NASA DAAC at the National Snow and Ice Data Center (http://nsidc.org/data/nsidc-0477.html); these data include a variety of file formats including HDF5 and searchable metadata. The FT-ESDR is projected in a global cylindrical Equal-Area Scalable Earth (EASE) grid, Version 1 format (Brodzik and Armstrong 2002) consistent with the format of the underlying SMMR, SSM/I(S) and AMSR-E/2 global T_b records used as primary inputs for the FT classification.

III. FT-ESDR version 4.0 changes from prior releases

The FT-ESDR Version 4.0 product effectively replaces earlier product releases (V3.0; Kim et al., 2014c). The Version 4.0 product contains the following changes from earlier product versions, and are designed to improve product coverage, accuracy and performance:

- A longer FT data record is represented, extending from 1979 to 2016 (38-years);

- A larger FT-ESDR global classification domain encompasses all land areas affected by seasonal frozen temperatures, including urban, snow-ice dominant, open water body dominant, and barren land. Open water areas included in the FT classification represent grid cells where the fractional surface water (*fw*) cover is less than 100% of the cell;

- A modified seasonal threshold algorithm (MSTA) is used for the FT classification where MSTA T_b reference FT conditions are calibrated annually for each pixel using ERA-Interim (Dee et al., 2011) daily surface air temperature (SAT) records;

- Detailed quality control (QC) flags are included in the product granules identifying grid cells and days with missing and interpolated T_b observations, and characterizing extensive open water bodies, complex terrain, and precipitation events;

- Updated annual data quality assurance (QA) maps are included indicating product performance and reliability.

The Version 4.0 FT-ESDR has greater spatial and temporal coverage than earlier FT-ESDR versions (Kim et al., 2014c), especially over boreal and arctic land areas with extensive open water cover that were previously screened from earlier FT classifications (Kim et al. 2011).

IV. FT-ESDR accuracy and performance

The Version 4.0 FT-ESDR release is developed by merging SMMR, SSM/I, and SSMIS 37 GHz frequency, vertical (V) polarization T_b records, and applying similar protocols used to construct earlier FT-ESDR product versions (Kim et el. 2011, 2012, 2014c). The FT-ESDR extends from 1979 to 2016 over a global classification domain and has been verified against a range of other independent FT metrics, including daily surface air temperature (SAT) records from global weather stations, *in situ* lake and river ice phenology records, and satellite observations of Greenland surface ice melt (Kim et al., 2017). The FT-ESDR product accuracy is primarily assessed in relation to daily SAT maximum (SAT_{max}) and minimum (SAT_{min}) values from the global WMO weather station network (4,234±706 [temporal-SD] stations); mean annual FT spatial classification accuracies are approximately 90.4 ±1.4 [inter-annual SD] and

84.4 ±1.6 [inter-annual SD] percent for respective FT-ESDR PM and AM retrievals over the global domain and long-term record. The AMSR (AMSR-E and AMSR2) portion of the FT-ESDR has similar spatial classification accuracy, but extends over a shorter (2002-2016) record encompassed by the AMSR-E and AMSR2 operational period. The FT-ESDR classification accuracy shows strong seasonal and annual variability, and is generally lower during active FT transition periods when spatial heterogeneity in landscape FT processes is maximized in relation to the relatively coarse (~25-km) satellite footprint (Kim et al. 2017). Global daily FT spatial classification accuracy is defined for each product daily granule from pixel-wise comparisons of FT classification accuracy in relation to co-located global weather station network daily air temperature (SAT_{min}, SAT_{max}) measurements (Kim et al. 2017); spatial classification accuracy is expressed as the proportion of global stations where the daily FT classification is consistent with station SAT measurement based FT estimates. Other data quality (QA) metrics are included that provide more spatially explicit information on algorithm performance, including potential negative impacts from open water cover, terrain complexity, length of FT transitional season, and MSTA FT threshold uncertainty influencing mean annual classification accuracy. Additional quality control (QC) flags identify other factors potentially affecting FT classification accuracy. The QC flags are spatially and temporally dynamic, and assigned on a per grid cell basis to denote missing satellite T_b records that are subsequently gap-filled through temporal interpolation of adjacent successful T_b retrievals prior to the FT classification. The QC flags also distinguish grid cells with large fractional open water areas (fw>0.20) and extreme elevation gradients (>300m), and days with large precipitation events (Ferraro et al., 1996).

V. FT algorithms:

   The FT-ESDR classification involves a modified seasonal threshold algorithm approach (MSTA) with radiometric T_b time-series that identify FT transition sequences by exploiting the dynamic T_b temporal response to differences in the aggregate landscape dielectric constant that occur as the landscape transitions between predominantly frozen and non-frozen conditions. These techniques are well-suited for resolving daily FT state dynamics rather than single events or seasonally dominant transitions (Kim et al. 2011). The Version 4.0 product uses the MSTA to classify daily (AM and PM) FT status from 37 GHz (V-pol) T_b time series from SMMR,

6

SSM/I(S) and AMSR records. The MSTA FT threshold was defined annually using an empirical linear regression relationship between the satellite T_b retrievals and daily ERA-Interim SAT estimates established for each grid cell. The FT thresholds were derived separately for the satellite T_b time series from AM and PM overpasses and using corresponding daily SAT minimum (SAT_{min}) and maximum (SAT_{max}) values. Larger weighting of SAT values closer to 0°C was used in selecting the corresponding T_b based FT threshold for each grid cell; weighting of the SAT and T_b regression relationship was derived using a cosine function within a temperature range extending from -60.0°C to 30.0°C and representing 99 percent of the SAT frequency distribution defined from the 36-year ERA-Interim SAT global climatology (Kim et al., 2017). An advantage of the MSTA relative to an earlier seasonal threshold algorithm (STA) based FT classification (Kim et al. 2011) is that the T_b threshold selection does not depend on frozen and non-frozen reference states derived by averaging T_b measurements over respective winter and summer periods, and is less sensitive to T_b data gaps during these reference periods.

VI. Ancillary data used for the FT-ESDR

We used daily SAT records from ERA-Interim global model reanalysis for pixel-wise annual calibration the MSTA FT thresholds. The global reanalysis data were also used to define the global FT-ESDR domain (**Figure 1**) using a simple SAT driven bioclimatic index (Kim et al. 2011) that identified all land areas where seasonally frozen air temperatures are a major constraint to ecosystem processes and land surface water mobility.
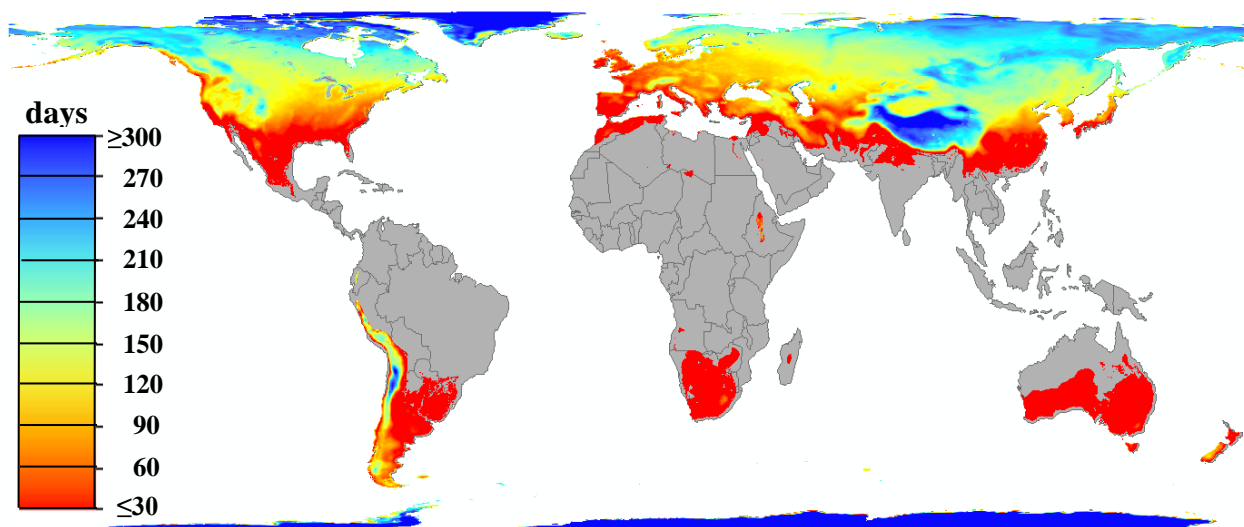
Independent daily SAT observations from global in situ WMO weather station measurements were used for verification of FT-ESDR daily accuracy. A simple zero degree Celsius temperature threshold was used to classify frozen and non-frozen temperatures from the SAT measurements; these results were then compared against the FT-ESDR daily classification results from the overlying grid cell. The resulting global FT spatial classification accuracy from all WMO stations was then summarized on a daily basis.

A global QA map is defined for each year of record and provides a discrete, grid cell-wise indicator of relative FT-ESDR quality that accounts for potential negative impacts from open water cover, terrain complexity, length of FT transitional season, and MSTA FT threshold uncertainty influencing mean annual FT classification accuracy indicated from the WMO station comparisons. The resulting annual QA map for selected year 2012 is presented in **Figure 2** and shows regions of relative high to low quality. The QA values were stratified into a smaller set of discrete categories ranging from low (estimated mean annual FT classification accuracy $< 70\%$) to best ($> 95\%$) quality. Mean proportions of the four QA categories encompass 54.1% (best), 36.0% (good; 85-95% agreement), 6.6% (moderate; 75-85% agreement), and 3.3% (low) of the global FT-ESDR domain for 2012.
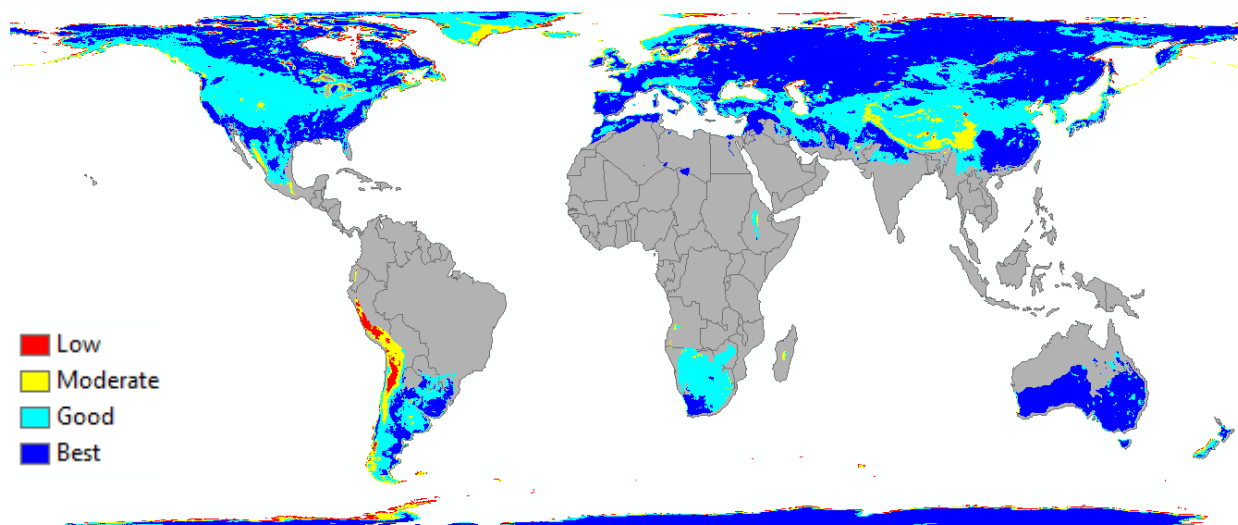

Figure 2: FT-ESDR annual quality assurance (QA) map for 2012, aggregated into low

(estimated mean annual spatial classification agreement < 70%), moderate (75-85%), good (85-95%) and best (>95%) relative quality categories. Land areas outside of the FT-ESDR domain are denoted by grey shading. (Adapted from Kim et al., 2017).

VII. Hierarchical data archive structure and available software tools:

Prior University of Montana FT-ESDR deliveries consisted of the data hosted on an NTSG FTP service. This FT-ESDR V4.0 delivery consists of a set of "tar" archive files, intended for NASA NSIDC personnel to use in constructing a data distribution point at NSIDC. The tar archives and related delivery files consist of the following files as documented in **Table 1** below. The data includes global daily FT classification files in HDF5 and GeoTIFF formats; daily FT accuracy and annual QA maps and supporting FT-ESDR documentation and software tools.

Table 1. Tar archive files encompassing the FT-ESDR (4.0) delivery.

FT-ESDR 4.0 Summary of NTSG Data Service Site	
[1]Directory	Summary of Contents
DAILY_HDF5	Multi-year record of global daily HDF5 science granules
DAILY_GIF	Multi-year record of global daily browse images (GIF format) for quick visual evaluation
QA_ACCURACY	Daily FT-ESDR mean global classification accuracy (%) and annual QA metadata in HDF5 file formats
TAR_ARCHIVES	Compressed tar files (*.tar.gz) FT gridded (global EASE-grid) data files archive for distribution and network transfer
MD5	MD5 checksum hash signatures for each FT file in the collection
DOC_V4	FT-ESDR database documentation files
TOOLS	File viewing software, including Panoply (v3.1.5) and HDFView (v2.8) for HDF5 (on MacOS,windows, Linux platforms)

[1]*Note that within a given directory tree such as DAILY_HDF5, where there are two sub-trees for the different sensor FT records ("./AMSR", and "./SMMR_SSMI"), a series of year-wise directories (2002-2016 or 1979-2016) occur below each of these.*

Two commonly available software tools are available through the FT-ESDR project and are routinely used with the HDF5 and GeoTIFF file formats this FT-ESDR distribution is produced in; these are HDFView and Panoply. Of course, other tool environments are also commonly used, such as ArcGIS, IDL/ENVI, MatLAB, as well as "R" (rhdf) and various Python

implementations (e.g. h5py and GDAL for Python) that support user developed code. Users of the HDF Groups hdfview utility should consult the following URL for additional information regarding their specific platform since there are distinctions in the binary distributions offered based on the user's operating system (e.g. whether it is 32 or 64 bit, etc.):
https://support.hdfgroup.org/products/java/release/download.html

VIII. Data format and file naming convention:

The FT data are stored in unsigned 8-bit integer data format as follows, shown with the GIF browse image color mapping scheme used (**Table 2**).

Table 2. FT-ESDR 8-bit integer data identifiers, with associated RGB colors used in the GIF browse images.

Classification		Browse Image Color Table		
	FT DN	R	G	B
Frozen (AM/PM frozen)	0	000	000	255
Thawed (AM/PM thawed)	1	255	000	000
Transitional (AM frozen and PM thawed)	2	168	168	000
Inverse Transitional (PM frozen and AM thawed)	3	076	230	000
No FT status available	252	250	250	250
Non-cold constraint area	253	255	255	255
100% open water	254	204	255	255
Fill value	255	255	255	255

Each FT-ESDR grid cell is projected in a global EASE-Grid 1.0 format (Armstrong & Brodzik, 1995; Brodzik and Armstrong 2002) at 25km spatial resolution, with 1383 columns and 586 rows consisting of 8-bit byte data type, for a total of 810438 pixels per daily data product. An ESRI projection file is included with the GeoTIFF files to aid in viewing the data in ArcMap. The geographical range of the FT-ESDR product is global, extending from -179.9999^o to 179.9999 ^{o} longitude and from -86.7167^o to 86.7167^o latitude.

The FT-ESDR includes dynamic quality control (QC) flags that are identified within an 8-bit character field for each grid cell as summarized below (**Table 3**). The first QC bit flag value (0) identifies whether actual T_b retrievals or interpolated T_b values were used for the daily FT classification. The second bit flag (1) denotes cells with a large spatial fraction of open water cover (fw > 20%), which is consistent with the fw threshold used for prior FT-ESDR releases (Kim et al., 2011). The third bit flag (2) denotes grid cells with a large elevation gradient (>300m), defined as the spatial standard deviation of the elevation distribution within each 25-km FT-ESDR grid cell, and derived from a global digital elevation map. The fourth bit flag (3) identifies large daily precipitation events occurring within a grid cell, and defined using a T_b threshold approach (Ferraro et al., 1996).

Table 3. Summary of FT-ESDR grid cell-wise Quality Control (QC) bit flags.

QC bit	Description (flagged=1, non-flagged=0)
0	flagged as 1 in case of interpolated T_b, otherwise set to 0
1	flagged as 1 in case of large open water fraction (>20%), otherwise set to 0
2	flagged as 1 in case of large elevation gradient (>300m), otherwise set to 0
3	flagged as 1 in case of large precipitation events, otherwise set to 0
4-7	bits unused

Each daily FT file consists of 3 separate granules, including: morning overpass (AM), afternoon overpass (PM) and combined daily AM and PM (CO) classification results. The FT product naming protocol follows these conventions:

[InstrumentLabel]_[Channel][Polarization]_[OverpassCode]_FT_[Year]_day[DOY].bin

For example, the file "SSMI_37V_CO_FT_2014_day365.bin" represents SSM/I and SSMIS sensor, 37 GHz, vertically polarized T_b based FT classification for composite daily conditions for day (calendar year) 365.

IX. Data Organization and Volume:

The daily FT data is organized in this collection first by instrument label, and then by year, with the AM, PM and CO granules stored in each annual directory. The FT-ESDR file sizes vary depending on the particular format option selected (**Table 4**). The FT-ESDR is also offered as a collection of matching HDF5 granules, which include an embedded FT classification legend, QC flags, production metadata, pixel statistics and frequency counts for the granule, and CF

convention style coordinate geolocation variables (cell_lat, cell_lon) to aid viewing. In addition to the primary FT data, detailed product quality information is also provided that includes granule level total mean spatial classification accuracy for the global domain defined on a daily basis (defined from pixel-wise comparisons against co-located global weather station SAT observations), and spatially contiguous relative data quality (QA) maps updated for each annual cycle. The FT-ESDR consists of a total of 57570 daily global 25km resolution granules, for a total of 18.8 Gb (HDF5 form) for all FT products. For faster downloading, compressed ("gzip") yearly FT binary files are provided in the "DAILY_TAR_ARCHIVES" directory.

Table 4. FT-ESDR file size summaries for HDF5 files.

Instrument	N. files	Range of Years	HDF5 Files	
			Kb	Gb
SMMR	8766	1979 – 1986	2863524	2.8 Gb
SSM/I and SSMIS	32874	1987 – 2016	10733128	11.0 Gb
AMSR-E and AMSR2	15930	2002 – 2016	5173464	5.0 Gb
Totals:	57570	38	18770116	18.8 Gb

A number of compressed tar archives (**Table 5**) are also available (see DAILY_TAR_ARCHIVES directory) as a convenient method for users to access related collections of the FT- ESDR files. Their names, manifests (table of content files), number of files, and data volume sizes are documented in the table below:

Table 5. FT-ESDR compressed tar file (tar.gz) archives and file sizes available for download.

Tar Archive Name	N. Files	Size
FT_V4_HDF5_SMMR_SSMI_Deliv.tar.gz	41640	4.7 Gb
FT_V4_HDF5_AMSR_Deliv.tar.gz	15930	1.8 Gb
FT_V4_HDF5_ANNUAL_ACC_Deliv.tar	112	6.5 Mb
FT_V4_HDF5_QA_Deliv.tar.gz	106	54 Mb
FT_V4_GeoTIFF_AMSR_Deliv.tar.gz	15930	433 Mb
FT_V4_GeoTIFF_SMMR_SSMI_Deliv.tar.gz	41640	1.2 Gb
FT_V4_GIF_SMMR_SSMI_Deliv.tar.gz	41640	2.3 Gb
FT_V4_GIF_AMSR_Deliv.tar.gz	15930	856 Mb

X. Example FT Figures:

The FT-ESDR provides a daily (CO) classification of the predominant landscape frozen or non-frozen status for each grid cell within the global domain (**Figure 3**). Four discrete FT metrics are distinguished from the AM and PM T_b retrievals, including frozen (both AM and PM overpasses), non-frozen (AM and PM), transitional (AM frozen, PM non-frozen) and inverse-transitional (AM non-frozen, PM frozen) states.
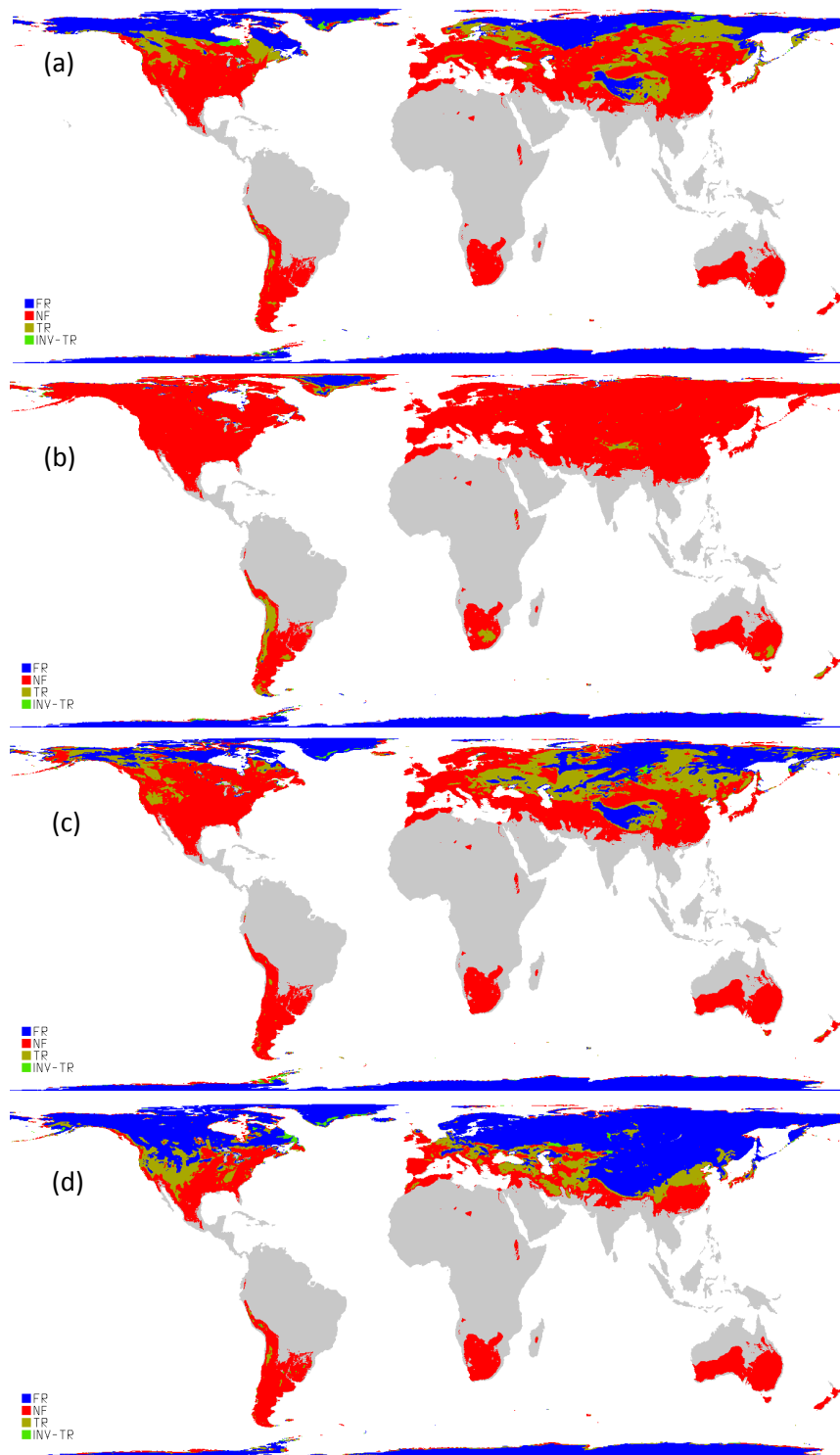
Figure 3: *Selected daily combined (CO) FT-ESDR classification results for 2014, where: (a) DOY (Day of Year) =100, (b) DOY=200, (c) DOY=300, and (d) DOY=360; white and grey colors denote respective open water bodies and land areas outside of the FT-ESDR domain; FR (AM and PM frozen), NF (AM and PM thawed), TR (AM frozen and PM thawed) and INV-TR (AM thawed and PM frozen).*

XI. References:

Armstrong, R. L. and M. J. Brodzik. 1995. An Earth-Gridded SSM/I Data Set for Cryosphere Studies and Global Change Monitoring. *Advances in Space Research*. 16, 155-163.

Armstrong, R., K. Knowles, M. Brodzik, and M.A. Hardman, 1998, updated 2012. DMSP SSM/I-SSMIS Pathfinder Daily EASE-Grid Brightness Temperatures. Version 2 [1987-2012]. Boulder, Colorado USA: NASA DAAC at the National Snow and Ice Data Center (http://nsidc.org/data/nsidc-0032.html).

Brodzik, M. J. and R. L. Armstrong. 2002. EASE-Grid: A versatile set of equal-area projections and grids. In M. Goodchild (Ed.), Discrete Global Girds. Santa Barbara, California USA: National Center for Geographic Information and Analysis.

Dee, D. P., S. M. Uppala, A. J. Simmons, P. Berrisford, P. Poli, S. Kobayashi, U. Andrae, M. A. Balmasewda, G. Balsamo, P. Bauer, P. Bechtold, A. C. M. Beljaars, L. van de Berg, J. Bidlot, N. Bormann, C. Delsol, R. Dragani, M. Fuentes, A. J. Geer, L. Haimberger, S. B. Healy, H. Hersbach, E. V. Holm, L. Isaksen, P. Kallberg, M. Kohler, M. Matricardi, A. P. McNally, B. M. Monge-Sanz, J. J. Morcrette, B. K. Park, C. Peubey, P. de Rosnay, C. Tavolato, J. N. Thepaut, and F. Vitart. (2011). The ERA-Interim reanalysis: configuration and performance of the data assimilation system. *Quarterly Journal of the Royal Meteorological Society*, 137, 553-597.

Du, J., J. S. Kimball, and L. Jones. (2015). Satellite Microwave Retrieval of Total Precipitable Water Vapor and Surface Air Temperature Over Land from AMSR2. *IEEE Transactions on Geoscience and Remote Sensing*, 53 (5), 2520-2531.

Du, J., J. S. Kimball, J. Shi, L. A. Jones, S. Wu, R. Sun, and H. Yang. (2014). Inter-calibration of satellite passive microwave land observations from AMSR-E and AMSR2 using overlapping FY3B-MWRI sensor measurements. *Remote Sensing*, 6, 8594-8616.

Ferraro, R. R., F. Weng, N. C. Grody, and A. Basist. (1996). An eight-year (1987-1994) time series of rainfall, clouds, water vapor, snow cover, and sea ice derived from SSM/I measurements. *Bulletin of the American Meteorological Society*, 77(5), 891-905.

Friedl, M. A., D. K. McIver, J. C. F. Hodges, X. Y. Zhang, D. Muchoney, A. H. Strahler, C. E. Woodcock, S. Gopal, A. Schneider, A. Cooper, A. Baccini, F. Gao, and C. Schaaf (2002). Global land cover mapping from MODIS: algorithms and early results. *Remote Sensing of Environment*, 83, 287-302.

GLOBE Task Team and others (Hasting, D. A., P. K. Dunbar, G. M. Elphingstone et al.). (1999). The global land one-kilometer base elevation (GLOBE) digital elevation model, version 1.0. National Oceanic and Atmospheric Administration, National Geophysical Data Center, 325 Broadway, Boulder, Colorado 80305-3328, U.S.A. Digital data base on the World Wide Web (http://www.ngdc.noaa.gov/mgg/toto/globe.html) and CD-ROMs.

Imaoka, K.; Takashi, M.; Misako, K.; Marehito, K.; Norimasa, I.; Keizo, N. (2012). Status of AMSR2 instrument on GCOM-W1, earth observing missions and sensors: Development, implementation, and characterization II. Proc. SPIE 2012, 852815, doi:10.1117/12.977774

JAXA. Digital media (https://gcom-w1.jaxa.jp).

Jones, L.A., and J.S. Kimball, 2010, updated 2012. Daily Global Land Surface Parameters Derived from AMSR-E, Version 1.1. Boulder Colorado USA: National Snow and Ice Data Center. Digital media (http://nsidc.org/data/nsidc-0451.html).

Kim, Y., J. S. Kimball, J. Glassy, and J. Du. (2017). An Extended Global Earth System Data Record on Daily Landscape Freeze-Thaw Determined from Satellite Passive Microwave Remote Sensing, *Earth System Science Data*, 9 (1), 133-147.

Kim, Y., J. S. Kimball, D. A. Robinson, and C. Derksen. (2015). New satellite climate data records indicate strong coupling between recent frozen season changes and snow cover over high northern latitudes. *Environmental Research Letters*, 10, 084004.

Kim, Y., J. S. Kimball, K. Zhang, K. Didan, I. Velicogna, and K. C. McDonald (2014a). Attribution of divergent northern vegetation growth responses to lengthening non-frozen seasons using satellite optical-NIR and microwave remote sensing, *International Journal of Remote Sensing*, 10.1080/01431161.2014.915595.

Kim, Y., J. S. Kimball, K. Didan, and G. M. Henebry. (2014b). Responses of vegetation growth and productivity to spring climate indicators in the conterminous Unites States derived from satellite remote sensing data fusion. *Agricultural and Forest Meteorology*, 194, 132-143

Kim, Y., J. S. Kimball, J. Glassy, and K. C. McDonald (2014c). MEaSUREs Global Record of Daily Landscape Freeze/Thaw Status. Version 3. [1979-2011]. Boulder, Colorado USA: NASA DAAC at the National Snow and Ice Data Center. http://dx.doi.org/10.5067/MEASURES/CRYOSPHERE/nsidc-0477.003

Kim, Y., J.S. Kimball, K. Zhang, and K.C. McDonald, 2012. Satellite detection of increasing northern hemisphere non-frozen seasons from 1979 to 2008: Implications for regional vegetation growth. *Remote Sensing of Environment* 121, 472-487.

Kim, Y., J. S. Kimball, K. C. McDonald, and J. Glassy. 2011. Developing a Global Data Record of Daily Landscape Freeze/Thaw Status using Satellite Microwave Remote Sensing. *IEEE Transactions on Geoscience and Remote Sensing.* 49, 3, 949-960.

Knowles, K., M. Savoie, R. Armstrong, and M. Brodzik, 2006, updated 2011. AMSR-E/Aqua Daily EASE-Grid Brightness Temperatures [2002-2011]. Boulder, Colorado USA: NASA DAAC at the National Snow and Ice Data Center (http://nsidc.org/data/nsidc-0301.html).

Knowles, K., E.G. Njoku, R. Armstrong, and M. Brodzik, 2000. Nimbus-7 SMMR Pathfinder Daily EASE-Grid Brightness Temperatures [1979-1987]. Boulder, Colorado USA: NASA DAAC at the National Snow and Ice Data Center (http://nsidc.org/data/nsidc-0071.html).

McDonald, K.C, and J.S. Kimball, 2005. Hydrological application of remote sensing: Freeze-thaw states using both active and passive microwave sensors. Encyclopedia of Hydrological Sciences. Part 5. Remote Sensing. M.G. Anderson and J.J. McDonnell (Eds.), John Wiley & Sons Ltd. DOI:10.1002/0470848944.hsa059a.

Park, H., Y. Kim, and J. S. Kimball. (2016). Widespread permafrost vulnerability and soil active layer increases over the high northern latitudes inferred from satellite remote sensing and process model assessments. *Remote Sensing of Environment*, 175, 349-358.

Yang, H., F. Weng, L. Lv, N. Lu, G. Liu, M. Bai, Q. Qian, J. He, H. Xu. (2011) The FengYun-3 microwave radiation imager on-orbit verification. *IEEE Transactions on Geoscience and Remote Sensing*, 49, 4552–4560.

Zhang, K., J.S. Kimball, Y. Kim, and K.C. McDonald, 2011. Changing freeze-thaw seasons in northern high latitudes and associated influences on evapotranspiration. Hydrological Processes 25, 4142-4151, DOI:10.1002/hyp.8350.